

Novel nanocomposites based on gelatin/HPET/chitosan with high performance acid red 150 dye adsorption

Ahmed A. Haroun · Hamada M. Mashaly ·
Nabil H. El-Sayed

Received: 5 June 2012 / Accepted: 9 August 2012 / Published online: 29 August 2012
© Springer-Verlag 2012

Abstract In this study, the properties of gelatin and chitosan are combined in the presence of hydrolyzed poly(ethylene terphthalate), HPET, and laponite to produce a novel hybrid natural-synthetic material for anionic dyes removal applications. Adsorption studies of acid red 150 from aqueous solution with respect to the initial dye concentration, temperature, time, pH, and sorbent dosage were investigated. The Langmuir adsorption model was applied to describe the equilibrium isotherms. The prepared nanocomposites were characterized using different techniques, such as FTIR, DSC, SEM, and TEM. The suitability of the adsorbent was tested by fitting the adsorption data with Langmuir isotherm. The results showed that the adsorption of AR150 was increased with an increasing in both of the dye and chitosan concentrations.

Keywords Gelatin · Chitosan · Poly(ethylene terphthalate) · Laponite · Acid red 150

Introduction

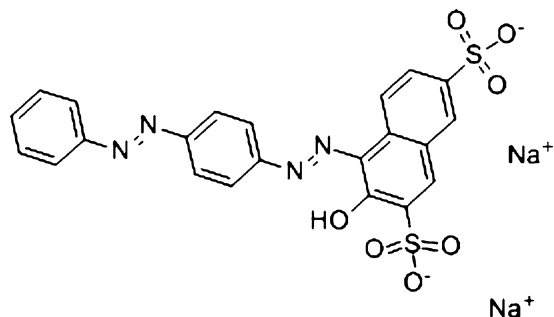
The textile industry is characterized by its high water consumption and is one of the largest producers of industrial wastewater. The main pollution sources of textile wastewater are the dyeing and finishing processes.

Wastewater containing dyes present a serious environmental problem because of its high toxicity and possible accumulation in the environment (Robinson et al. 2001; Mittal et al. 2006). Most of these dyes are synthetic and classified based on their chemical structures into different classes. The removal of the dyes from the textile effluents is currently of great interest and is a major issue, because of the difficulty of treating such water by conventional methods. Various physical and chemical treatment methods of the industrial wastewater have been suggested, that including adsorption methods, coagulation processes, photocatalytic degradation, and hypochlorite treatment (Behnajady et al. 2007; Gupta 2009; Rauf et al. 2007). The physical adsorption has been proven to be the most efficient method for quickly lowering the dissolved dyes concentration in an effluent. In this regard, activated carbon is the most widely used adsorbent for removal of dyes from the aqueous solution (Demirbas 2009; Luo and Zhang 2009). Furthermore, polymeric hydrogels play an important role in the treatment of waste water (Siddaramaiah et al. 2008). Chitosan is a partially deacetylated of the chitin. It has prospective applications in many fields such as waste water treatment, functional membranes, and flocculation (Pati and Nayak 2011). The adsorption of cationic dyes by polymer nanocomposites (NCs) hydrogels using an organic crosslinker was reported previously (Ekici et al. 2006). Poly(ethylene terphthalate), PET, is a thermoplastic resin and was first prepared in 1946. The hydrolysis of PET can be achieved in neutral, alkaline, and acid media and resulted in terphthalic acid and ethylene glycol (De Carvalho et al. 2006). Moreover, the partially hydrolysis products of PET were used as dye adsorbents in the treatment of effluents of the textile industry. Recently, some attempts have been made to prepare and investigate novel thermoplastic films and interpenetrating polymer network for removal some

A. A. Haroun (✉) · N. H. El-Sayed
Chemical Industries Research Division, National Research
Center, Cairo, Egypt
e-mail: haroun68_2000@yahoo.com

H. M. Mashaly
Dyeing and Printing Department, National Research Center,
Cairo, Egypt

heavy metal ions (Haroun and El-Halawany 2011; Haroun et al. 2010). The aim of this study was to prepare and characterize novel NCs based on gelatin/HPET/chitosan in addition to the adsorption study of AR150 was investigated.



Chemical structure of Acid Red 150 (AR 150)

Experimental

Materials

Acid dye red 150 was purchased from Ciba and used without further purification. Technical gelatin, faint yellow powder, which has bloom value 200, viscosity about 5.5 poise and ash 2.5 %, obtained from Al-Amin Co., Egypt. Laponite clay (laponite RD) was supplied from Rockwood Ind. and used as received. The clay powder has the chemical formula $(\text{Si}_{7.95}\text{Al}_{0.05})(\text{Mg}_{5.48}\text{Li}_{0.36}\text{Ti}_{0.01})\text{O}_{20}(\text{OH})_4 \text{K}_{0.01}$. All the other chemicals were purchased from Merck and used as received.

Synthesis of gelatin/HPET/chitosan nanocomposites

PET (5 g) was added to 50 mL of sulphuric acid (96 %) under reflux at 30 °C for 120 min. The product was filtered off, neutralized and washed thoroughly with distilled water. Hydrolyzed PET, HPET, was stirred with 2 mL triethanolamine then added to the mixture with different ratios of gelatin and chitosan aqueous solutions (1:1 and 1:2). Different concentrations of laponite (0, 0.05, and 0.2 wt%) and 0.5 wt% of potassium persulphate were sonicated for 5 min then subsequently added to the above mixture for 5 h at 70 °C. Glutardialdehyde (1 wt%) was added and further stirring for 1 h. The resultant products were filtered off washed thoroughly with 0.1 N sodium hydroxide and ethanol/water (1:1), respectively. The prepared NCs (denoted as I, II, III, and IV) were dried and kept for further investigations (Table 1).

Characterization

The nanocomposite samples were examined using Perkin-Elmer Fourier transform infrared spectroscopy under

Table 1 Chemical composition of the prepared NCs

Nanocomposites	Chemical compositions (wt%)			
	Gelatin	HPET	Chitosan	Laponite
I	1	1	1	0
II	1	1	1	0.05
III	1	1	1	0.2
IV	1	1	2	0.05

certain conditions such as: scan resolution 4 cm^{-1} , scan rate 2 mm s^{-1} , range 4,000–600 cm^{-1} , and mode transmission. Thermogravimetric analysis (TGA/DTA) of the nanocomposite samples were carried out using Perkin Elmer-7 series thermal analyzer at heating rate of 10.0 $^{\circ}\text{C min}^{-1}$ over the temperature range of 30–1,000 °C.

The structural features of the prepared nanocomposites were investigated at different magnification (X220 and X750) using JEOL-Scanning Electron Microscope (SEM). Before observation, the fractured surfaces were coated with Au using SEM coating device. Three micrographs were taken from different zones of each surface sample under investigation. The particle size of the prepared NCs was carried out with a JEOL transmission electron microscope JEM-1230 (TEM).

Batch adsorption experiments

Stock solution of AR150 was prepared without pH adjustment. About 0.3 g of NCs (I, II, III, and IV) and 50 mL of the standard solutions were placed in 250-mL beakers and stirred for a certain period. After filtration, the concentration of AR150 in supernatant was analyzed by an ultraviolet visible spectrophotometer (Schimadzu, Japan) with 2 nm resolution using calibration curve at λ_{max} 530 nm. The adsorption of AR150 was studied in pH range 3–9, through adjusting pH using either HCl or NaOH. The prepared NCs were equilibrated at a particular pH value for different time and temperature intervals (20, 40, 60, and 80) min and (40, 50, 60, and 70 °C), respectively, at constant shaking rate about 400 rpm min^{-1} . Adsorption equilibrium tests were conducted at optimum conditions. The adsorption capacity was calculated as follows:

$$Q_e = (C_0 - C_e)V/W, \quad (1)$$

where C_0 and C_e (mg L^{-1}) are the initial and the final or equilibrium AR150 concentration, V (mL) is the volume of the AR150 solution, and W (g) is the weight of the NC. The Langmuir adsorption isotherm is expressed as follows:

$$C_e/Q_e = (1/Q) C_e + 1/Qb, \quad (2)$$

where C_e and Q_e are the equilibrium dye concentrations in the aqueous (mg L^{-1}) and solid (mg g^{-1}) phases (adsorbed

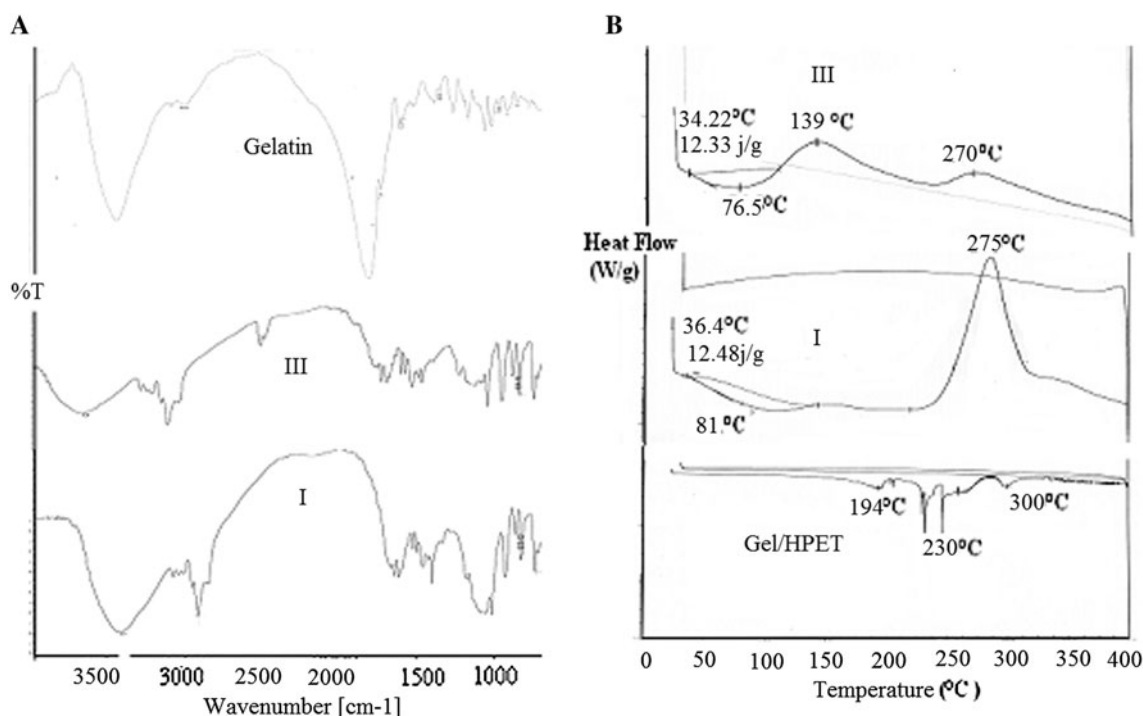


Fig. 1 a FTIR spectra and b DSC of the prepared NC (I and III), pure gelatin and gelatin/HPET

per unit weight of NC), respectively, b is the Langmuir adsorption equilibrium constant related to the affinity of binding sites (mL mg^{-1}) and is a measure of the energy of adsorption. While Q is the maximum adsorption at monolayer (mg g^{-1}). A linearized plot of C_e/Q_e against C_e gives b and Q . The essential features of the Langmuir isotherm can be expressed in terms of the dimensionless equilibrium parameter R_L , which defined as:

$$R_L = 1/(1 + bC_0), \quad (3)$$

where b is the Langmuir constant as described above and C_0 is the initial AR150 dye concentration (277 mg L^{-1}).

Effect of nanocomposites dosage

A 10 mL of dye of known concentration (0.5 g L^{-1}) and the different amounts of the four composite concentration ($0.1, 0.3, 0.5,$ and 0.8 g L^{-1}) were taken in a 50-mL Stoppard conical flask. This mixture was agitated at the optimum temperature values controlled by shaking water bath at a constant speed per minutes (rpm) for the optimum time value and at the optimum pH value. Samples were centrifuged using Research Centrifuge (Sigma, Germany) at 4,000 rpm for 15 min and analyzed for remaining dye concentration spectrophotometrically using UV-spectrophotometer.

Results and discussion

Physical characterization of the prepared nanocomposites

The physical property analyses of the gelatin/chitosan NCs are important in this study because the analyses give some insights of the effect of HPET and modified clay (laponite) to the natural chemical and physical properties of gelatin and chitosan. This information is very useful in elucidating the adsorption capacity of the adsorbents towards anionic dyes. The FTIR spectra of the prepared NCs (I and III) and pure gelatin are shown in Fig. 1. The spectrum of gelatin displays a number of adsorption peaks, an indication of different types of functional groups present in gelatin matrix. According to (Fatyeyeva et al. 2011) FTIR spectrum of pure Laponite is characterized by broad H–OH stretching and bending adsorption bands located at about $3,450$ and $1,633 \text{ cm}^{-1}$, respectively. Also, the peaks at $3,665$ and 455 cm^{-1} are attributed to the Mg–OH stretching vibration of the magnesium ion present in the octahedral sheet of the clay. Moreover, the peaks at $1,000 \text{ cm}^{-1}$ corresponds to the Si–OH stretching of silanol groups. Compared to the blank laponite, the FTIR spectrum of the NCs I and III. The SEM images in Fig. 2a show the

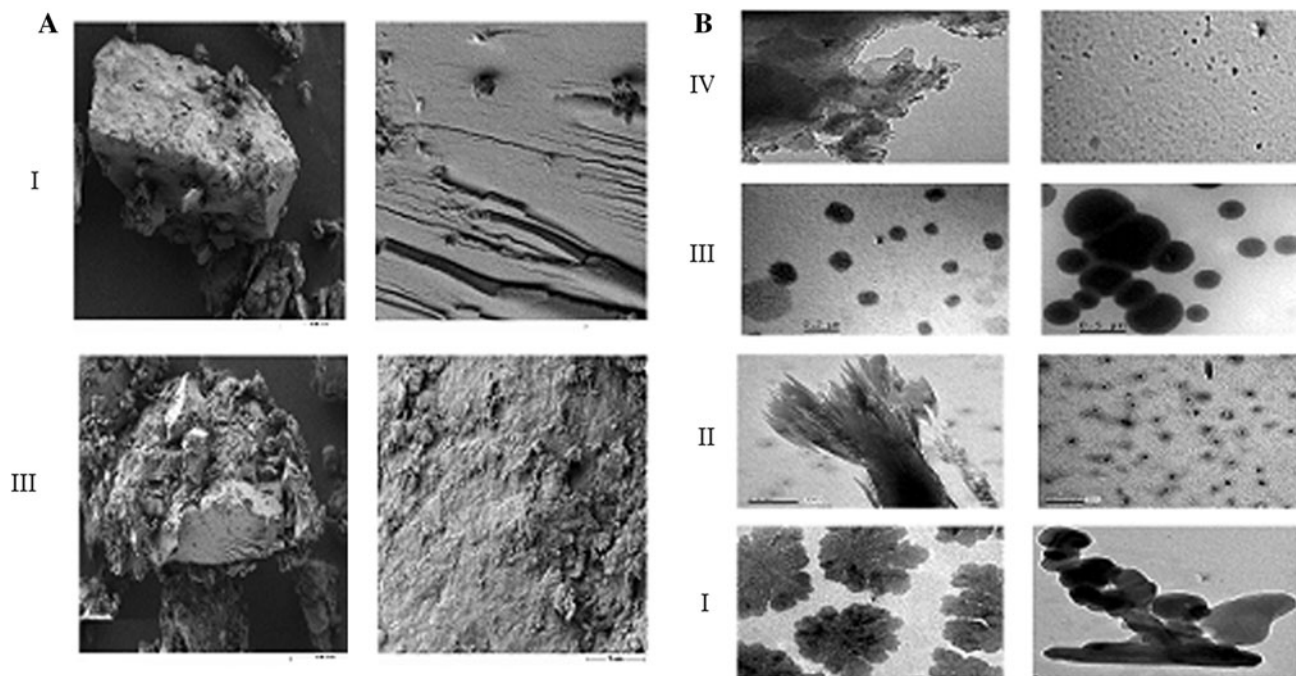


Fig. 2 a SEM-micrographs and b TEM images of the prepared NC (I, II, III, and IV), at gelatin/chitosan molar ratios (1:1 and 1:2), 1 wt% HPET, laponite conc (0, 0.05, and 0.2 wt%)

significant morphological difference of the surfaces between NCs I and III. The NC III which contains the modified clay (laponite), displays rough surface structure in comparison with NC I.

Effect of initial pH

Figure 3a shows the effect of pH on adsorption percentage (%) of AR150 onto the different NC. The pH affects significantly the adsorption capacities of AR150 onto the different NC. In general, the uptakes are much higher in acidic solutions than those in neutral and alkaline conditions. According to (Yoshida et al. 1993; Kumar 2000), at lower pH more protons will be available to protonate amine groups of chitosan and/or gelatin molecules to form $-(NH_3)^+$, thereby increasing electrostatic attractions between negatively charged dye anions and positively charged adsorption sites and causing an increase in dye adsorption. This explanation agrees with our data on pH effect. It can be seen that the pH of aqueous solution plays an important role in the adsorption of acid dye (AR150) on the prepared NC Scheme 1.

Effect of contact time

Figure 3b shows the effect of time on adsorption percentage (%) of AR150 onto the different NC. The effect of contact time on dye sorption on target NCs was studied for

duration of 20–80 min. In case of the NC IV, the percent sorption of dye gradually increased with time from 20 to 80 min. While, in case of the NCs (I, II, and III), the percentage sorption of AR150 did not change with increase of time.

Effect of temperature

Figure 3c shows the effect of temperature on adsorption of AR150 onto the different NC at pH 3.0, time 40 min, and dye concentration 500 mg L^{-1} . The increase in temperature from 40 to 70 °C leads to an increasing in dye uptake. After equilibrium, the increase in dye uptake indicates the endothermic nature of adsorption (Gurses et al. 2006).

Effect of adsorbent dosage

Figure 3d shows the adsorption percentage (%) of AR150 onto the different NC at pH 3.0, 40 °C, and 40 min. The percentage increases significantly with an increasing in the adsorbent dosage from 0.1 to 0.6 g. Increasing the adsorbent dosage at fixed AR150 concentration provided more available adsorption sites for AR150 and thus increased the extent of AR150 uptake.

Effect of initial dye concentration

Figure 4 shows the effect of initial dye concentration on the adsorption percentage of the different NC at pH 3,

Scheme 1 Removal of AR150 from aqueous medium using the prepared NCs

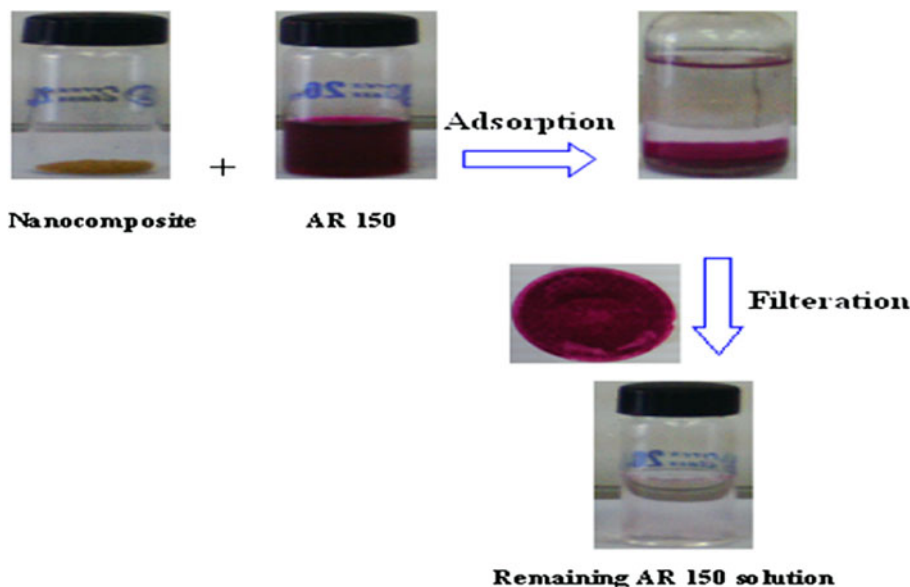
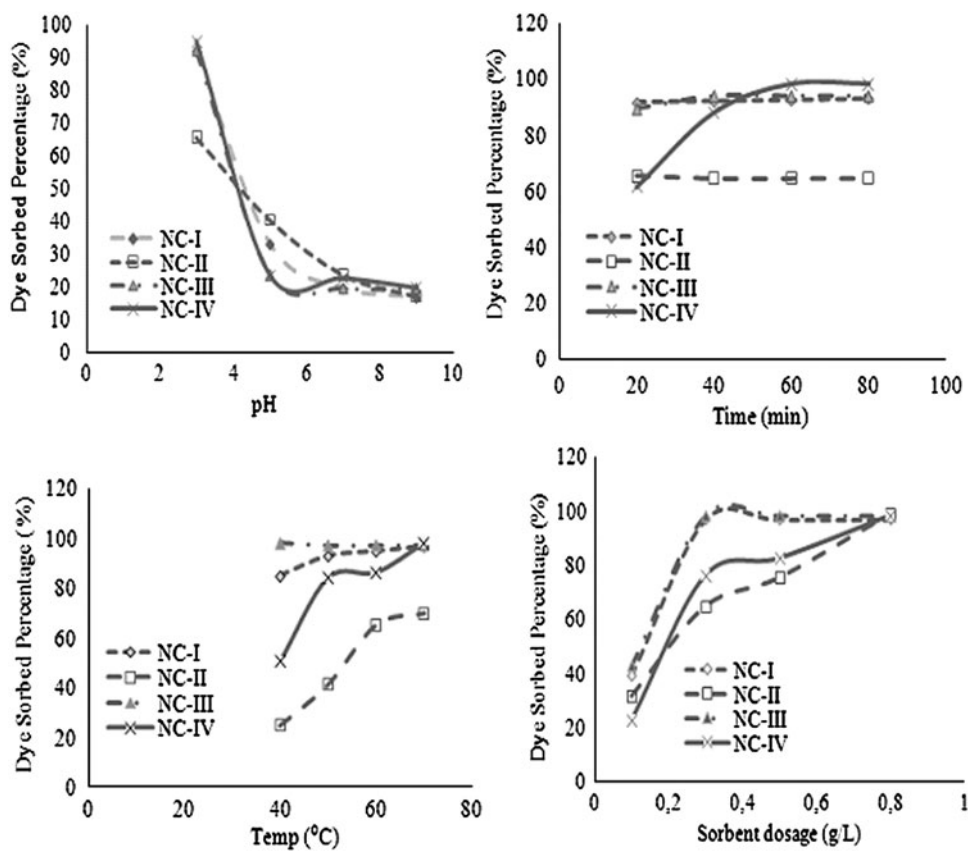


Fig. 3 Effect of **a** pH, **b** time, **c** temperature, and **d** sorbent dosage of the prepared NC (*I, II, III, and IV*), at constant dye concentration 500 mg L^{-1} and shaking rate 400 rpm min^{-1}



40 °C, and 40 min. In case of NC I and II, an increasing in initial dye concentration leads to an increase in the adsorption capacity of AR150 on NC. While, in case of NC III and IV, the adsorption (%) was decreased with an increasing of the initial dye concentration. This indicates

that both of the initial dye concentrations and the composition of the NC play an important role in the adsorption capacities of AR150 on the different NC. In other words, dye molecules can migrate from the external surfaces to the interlamellar region, resulting in the disaggregation of the

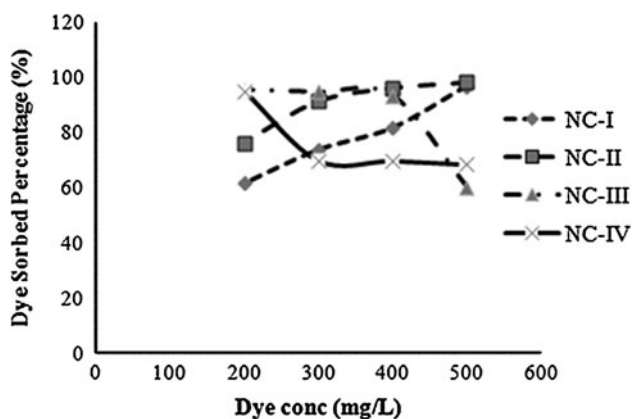


Fig. 4 Effect of AR150 dye concentration on the adsorption rate of the prepared NC (I, II, III, and IV), at constant NC dose 0.3 g, pH 3.0, temperature 40 °C, and time 40 min

aggregates and restoring the monomers. At high load rates of AR150, agglomerates are expected to be predominant, while monomers and dimmers are practically absent in AR150–NC complex (Bujdak and Komadel 1997).

Adsorption kinetics

Kinetics of adsorption is important parameter to evaluate an adsorption dynamics and examine the efficiency of the adsorption process. Also, study of equilibrium adsorption isotherm is fundamental in describing the interactive behavior between the adsorbate and the adsorbent and is

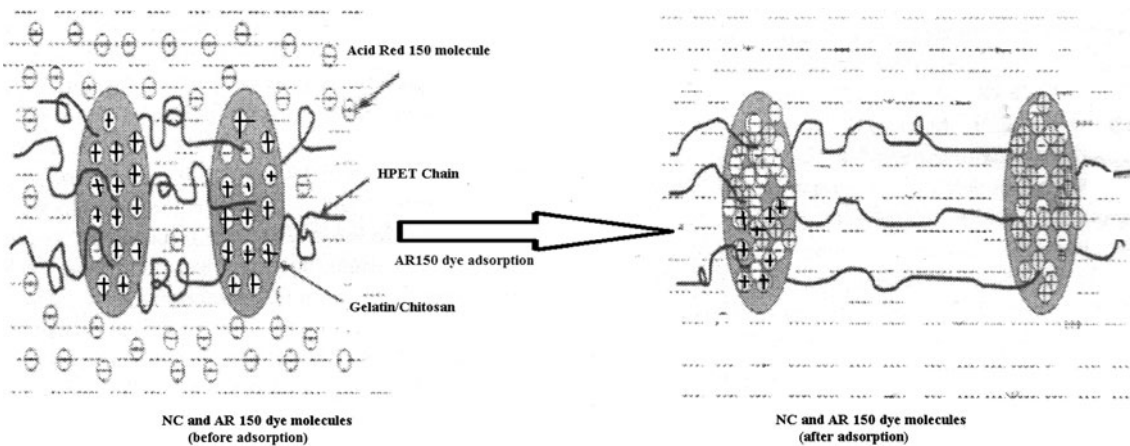
important in designing an adsorption system. The calculated results of the most widely used Langmuir equation, which is valid for monolayer sorption on to a surface with a finite number of identical sites, are given in Table 2. As can be seen in Table 2, amount of AR150 adsorbed by NC I and IV (909 and 625 mg g⁻¹, respectively) was relatively higher than that in case of NC II and III (526 and 556 mg g⁻¹, respectively). This might be due to the higher number of cationic groups, $-(NH_3)^+$, in NC I due to the absence of laponite (0 wt%) in comparison with that in case of NC II and III (0.05 and 0.2 wt%, respectively). On the other hand, NC IV contains relatively higher content of chitosan (2 wt%), in spite of the presence of laponite. According to (Cestari 2008), the adsorption of anionic dye occur mainly due to the electrostatic interaction between amine groups of the chitosan, $-(NH_3)^+$, and the $-(SO_3)^-$ groups of the anionic dyes. It is found that the adsorption of AR150 on NC was correlated well ($R^2 = 0.94$) with the Langmuir equation under the concentration range studied. A similar adsorption isotherm was obtained in the studies carried out by Cheung et al. (2007, Wang and Wang (2008), Zubieta et al. (2008), and Annadurai (2008). It has been reported that the effect of isotherm shape with a view to predict it an adsorption system is favorable or unfavorable. R_L values within the range $0 < R_L < 1$ indicate favorable adsorption. R_L values calculated using C_0 as high as 277 mg L⁻¹ are well within the defined range (Table 2) and indicate the acceptability of the process (Sujoy et al. 2006). It is also important to compare the value of maximum of adsorption

Table 2 Langmuir adsorption isotherm

Nanocomposites	Constants in Langmuir model			
	Q (mg g ⁻¹)	b (mL mg ⁻¹)	R_L (using $C_0 = 277$ mg L ⁻¹)	R^2
I	909	0.0007	0.838	0.9445
II	526	0.0009	0.801	0.9646
III	556	0.0036	0.501	0.9956
IV	625	0.0025	0.591	0.9959

Table 3 Comparison adsorption capacities of dyes on various low-cost adsorbents

Dyes	Adsorbent	Q (mg g ⁻¹)	References
Acid red 150	I	909	This study
	II	526	This study
	III	556	This study
	IV	625	This study
Acid red 37	Chitosan	357	Kamari et al. (2009)
Acid red 73		728	Wong et al. (2004)
Acid green 25		645	Wong et al. (2004)
Acid blue 13	<i>Murraya koenigii</i> seeds	53	Uresh et al. (2011)



Scheme 2 Proposed adsorption mechanism of AR 150 dye molecules on the prepared Ncs

capacity obtained from this study with values from other reported low-cost adsorbents as shown in Table 3. Probably the electrostatic interactions are needed only to transfer the dye ions to the nearest environment of the cationic polymer (gelatin/chitosan), later even their mechanical incorporation into NC accompanied by weak *Van der Waal's* dispersion forces seems to be a satisfactory reason for dye particles to be precipitated (Scheme 2). The conformational compatibility and adaptation of macromolecular chains and the dye in such processes are certainly of great importance. There is the probability that the forces moving in such “steric complexes” based on interpenetration and adaptation cannot be designated as “hydrophobic” in terms of their classical interpretation. Based on the above considerations, AR150 dye binding by a cationic flocculant in the presence of various anionic substances is a multi-step process (Zemaitaitiene et al. 2003) Scheme 2.

Conclusions

In this study, it was found that the sorption tends to attain the equilibrium in nearly 40 min. The maximum removal capacities for initial dye concentration, 277 mg L^{-1} , were 909, 625, 526, and 556 mg g^{-1} for the prepared NC I, II, III, and IV, respectively. According to Langmuir isotherm model, all the NCs exhibited favorable adsorption systems for the anionic dye (AR150) at concentrations $277\text{--}500 \text{ mg L}^{-1}$.

Conflict of interest The authors declare that they have no conflict of interest.

References

Annadurai G, Ling LY, Lee JF (2008) Adsorption of reactive dye from an aqueous solution by chitosan: isotherm, kinetic and thermodynamic analysis. *J Hazard Mater* 152:337–346

- Behnajady MA, Modirshhla N, Daneshvar N, Rabbani M (2007) Photocatalytic degradation of an azo dye in a tubular continuous-flow photoreactor with immobilized TiO_2 on glass plates. *Chem Eng J* 127:167–176
- Bujdak J, Komadel P (1997) Interaction of methylene blue with reduced charge montmorillonite. *J Phys Chem B* 101:9065–9068
- Cestari AR, Vieira EFS, Tavares AMG, Bruns RE (2008) The removal of the indigo carmine dye from aqueous solutions using cross-linked chitosan: evaluation of adsorption thermodynamics using a full factorial design. *J Hazard Mater* 153:566–574
- Cheung WH, Szeto YS, McKay G (2007) Intraparticle diffusion processes during acid dye adsorption onto chitosan. *Bioresour Technol* 98:2897–2904
- De Carvalho GM, Muniz EC, Rubira AF (2006) Hydrolysis of post-consume poly(ethylene terephthalate) with sulfuric acid and product characterization by WAXD, ^{13}C NMR and DSC. *Polym Degrad Stab* 91:1326–1330
- Demirbas A (2009) Agricultural based activated carbons for the removal of dyes from aqueous solutions: a review. *J Hazard Mater* 167:1–9
- Ekici S, Yasemin I, Dursun S (2006) Poly (acrylamide-sepiolite) composite hydrogels: preparation, swelling and dye adsorption. *Polym Bull* 57:231–241
- Fatheyeva K, Bigarre J, Blandel B, Galiano H, Gaud D, Lecardun M, Epailard F (2011) Grafting of P-styrene sulfonate and 1,3-propane sulfone onto laponite for proton exchange membrane fuel cell application. *J Membr Sci* 366:33–42
- Gupta VK, Suhas AB (2009) Application of low-cost adsorbents for dye removal—a review. *J Environ Manag* 90:2313–2342
- Gurses A, Dogar C, Yalcin M, Acikyildiz M, Bayrak R, Karaca S (2006) The adsorption kinetics of the cationic dye, methylene blue, onto clay. *J Hazard Mater B* 131:217–228
- Haroun AA, El-Halawany NR (2011) Preparation and evaluation of novel interpenetrating polymer network-based on newspaper pulp for removal of copper ions. *Polym Plast Technol Eng* 50:232–238
- Haroun AA, Abu Taleb EM, Abd El-Ghaffar MA (2010) Synthesis and characterization of novel thermoplastic films for removal of heavy metal ions. *Polym Plast Technol Eng* 49:454–461
- Kamari A, Ngah WSW, Liew LK (2009) Chitosan and chemically modified chitosan beads for acid dyes sorption. *J Environ Sci* 21:296–302
- Kumar MNVR (2000) A review of chitin and chitosan applications. *Reactive Funct Polym* 46:1–27
- Luo X, Zhang L (2009) High effective adsorption of organic dyes on magnetic cellulose beads entrapping activated carbon. *J Hazard Mater* 171:340–347

- Mittal A, Mittal J, Kurup L (2006) Adsorption isotherms, kinetics and column operations for the removal of hazardous dye, tartrazine from aqueous solutions using waste materials-bottom ash and de-oiled soya, as adsorbents. *J Hazard Mater* 136:567–578
- Pati MK, Nayak P (2011) Grafting vinyl monomers onto chitosan. IV. Graft copolymerization of acrylic acid onto chitosan using ceric ammonium nitrate as the initiator. Characterization and antimicrobial activities. *Mater Sci Appl* 2:1741–1748
- Rauf MA, Bukallah SB, Hamadi A, Sulaiman A, Hammadi F (2007) The effect of operational parameters on the photoinduced decoloration of dyes using a hybrid catalyst V_2O_5/TiO_2 . *Chem Eng J* 129:167–172
- Robinson T, McMullan G, Marchant R, Nigam P (2001) Remediation of dyes in textile effluent: a critical review on current treatment technologies with a proposed alternative. *Bioresour Technol* 77:247–255
- Siddaramaiah PL, Kim NH, Heo SB, Lee JH (2008) Novel PAAm/laponite clay nanocomposite hydrogels with improved cationic dye adsorption behavior. *Compos B* 31:756–763
- Sujoy DK, Jayati B, Akhil RD, Arun KG (2006) Adsorption behavior of rhodamine B on *Rhizopus oryzae* biomass. *Langmuir* 22:7265–7272
- Uresh SS, Ilfred RW, Ugumar S, Aiyalagan TM (2011) Adsorption of acid red 18 from aqueous solution onto activated carbon prepared from *Murraya koenigii* (curry tree) seeds. *Asian J Chem* 33:219–224
- Wang L, Wang A (2008) Adsorption properties of congo red from aqueous solution onto *N,O*-carboxymethyl-chitosan. *Bioresour Technol* 99:1403–1408
- Wong YC, Szeto YS, Cheung WH, McKay G (2004) Adsorption of acid dyes on chitosan—equilibrium isotherm analyses. *Process Biochem* 39:695–704
- Yoshida H, Okamoto A, Kataoka T (1993) Adsorption of acid dye on crosslinked chitosan fibers equilibria. *Chem Eng Sci* 48:2267–2272
- Zemaitaitiene RJ, Zliobaite E, Klimaviciute R, Zemaitaitis A (2003) The role of anionic substances in removal of textile dyes from solutions using cationic flocculant. *Colloids Surf A Physicochem Eng Aspects* 214:37–47
- Zubieta CE, Messina PV, Luengo C, Dennehy M, Pieroni O, Schulz PCJ (2008) Reactive dyes remotion by porous TiO_2 -chitosan materials. *Hazard Mater* 152:765–777